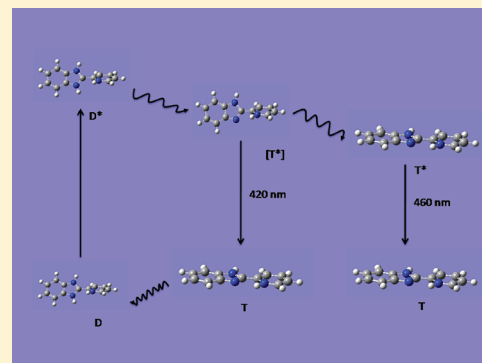


## 2-(2'-Pyridyl)benzimidazole as a Fluorescent Probe of Hydration of Nafion Membranes

E Siva Subramaniam Iyer, Dhruvajyoti Samanta, Arghya Dey, Aniket Kundu, and Anindya Datta\*

Department of Chemistry, Indian Institute of Technology Bombay, Mumbai, India 400076

**ABSTRACT:** 2,2'-(Pyridyl)benzimidazole is used as a probe to explore proton transfer through nafion membranes. The probe marks the availability of water in native as well as cation-exchanged membrane. Using steady state and time-resolved fluorescence studies, it has been shown that the rotation of the pyridyl and benzimidazole rings with respect to each other, which is ultrafast in higher water contents, is hindered as the water content in the membranes is decreased. In cation-exchanged membranes, it is observed that the formation of the ESPT (excited state proton transfer) state is reduced to a large extent. Thus, it may be inferred that the proton transport is observed to be hindered even in molecular dimensions of one water molecule thereby bolstering the contention that it may not be essential for water channels to break for proton conductivity to decrease.

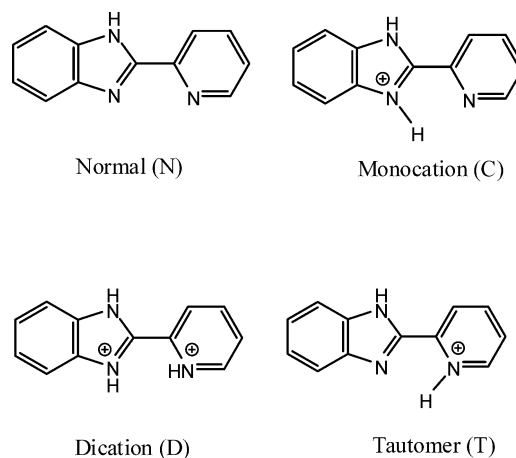


### ■ INTRODUCTION

Fuel cells operate by harnessing the energy released by the reaction of hydrogen and oxygen to yield water.<sup>1</sup> To achieve this purpose, compartmentalization of protons and hydroxide ions has to take place inside the fuel cell. This can be done by the use of a matrix that can preferentially transport either of the charged species. Nafion membranes, ethylpersulfonated Teflon polymers, prove to be a good material for this purpose.<sup>2,3</sup> These are negatively charged owing to the strongly acidic sulfonate groups and can retain high amounts of water. These two features have a combined effect on high and preferential proton conductivity in these membranes.<sup>4</sup> The membrane conductivity is influenced by various factors like temperature, water content, counterions present, and so forth.<sup>5–7</sup> The mechanism of water and proton transport in nafion remains an interesting issue of debate to date. It is important to understand the processes taking place in nafion to design more efficient and affordable membranes. It is widely believed that the sulfonate groups come together giving rise to pools of water, which are connected by channels (aka, cluster network model).<sup>8,9</sup> Another school of thought proposes parallel channels of varying diameters.<sup>7</sup> All of these models agree upon the fact that the nature of water is different from that of bulk water and behaves differently as the water content changes in the membrane. It is experimentally observed that the conductance of these membranes drops by several orders of magnitude as the water content in the membranes goes down.<sup>10</sup> The various models assign this phenomenon to the breaking up of water channels leading to a decrease in the conductivity of the membranes. Enormous amounts of literature are available in this context but none of them are highly conclusive. On the contrary, we have observed that the proton mobility, probed by the excited state proton transfer (ESPT) in protonated coumarin 102 is hindered even at molecular levels,<sup>11</sup> where the dimensions of proton transport

are much smaller than the established dimensions of water channels. We observe that interactions, other than the disruption of water channels, contribute significantly to the decrease in proton conductivity of nafion upon drying. Here, we try to explore the problem with another probe 2,2'-(pyridyl)benzimidazole (2PBI) used (Scheme 1). The molecule exists as a

**Scheme 1. Various Possible Species Involved in Photophysics of 2PBI; Note That Tautomer Is Formed Only in Excited State, It Does Not Exist in Ground State**



monocation, dication, or neutral form in the ground state depending upon the acidity of the environment and undergoes excited state intramolecular proton transfer to form a tautomer form in the excited state. This process is mediated by a water

**Received:** October 22, 2011

**Revised:** December 21, 2011

**Published:** January 5, 2012

bridge consisting of a single water molecule or by a hydrogen atom transfer from imidazole nitrogen to pyridyl nitrogen.<sup>12,13</sup> For the fluorescent probe Coumarin 102, we had observed that the proton transfer from the nitrogen end of the molecule to the oxygen end was hindered drastically as the water content in the membranes had been reduced. Exchange of  $\text{H}_3\text{O}^+$ , the counterion of the sulfonate groups, with cations like  $\text{Na}^+$  or  $(\text{CH}_3)_4\text{N}^+$  ions reduces the water content in the membrane; however, the probe could not sense the changes in the environment brought about by drying the cation-exchanged membranes. This happened because the dye existed in its neutral form and fluorescence was obtained from the electroneutral excited state and the medium was not acidic enough to protonate the coumarin. In 2PBI if the proton transfer is hindered, upon lowering water contents, then the observation would serve to support our contention that proton transport is affected even at the molecular level and that disruption of water channels is not the only factor that needs to be considered in the decrease of proton mobility at low hydration levels. Here, we have been able to observe the effect of drying in the cation-exchange membrane, which could not be sensed by our earlier experiments. The dye 2PBI helps to overcome the drawback of the coumarin probe as it marks the changes in environments in cation-exchanged membranes as well.

At this point, it would be useful to discuss the earlier reports of the spectral and temporal properties of 2PBI in aqueous solutions and microheterogeneous media. The absorption spectrum at pH 7 corresponds to the absorbance of the neutral (N) form of 2PBI. The monocation (C) where the other imidazole nitrogen is protonated also absorbs in the same region as the neutral form. The fluorescence maximum of the  $\text{N}^*$  and  $\text{C}^*$  appears around 360 nm. The dication is nonemissive. It is observed that in acidic pH in addition to a band at 360 nm a new band at 450 nm also arises. This has been assigned to a  $\text{T}^*$  arising from the  $\text{C}^*$  form. These assignments are supported by the  $\text{p}K_a$  and  $\text{p}K_a^*$  of various N atoms present in the molecule.<sup>14</sup> In aqueous medium of pH 2–7, the dication does not exist and the formation of  $\text{T}^*$  is suggested to be taking place from  $\text{C}^*$ . The mechanism is believed to be taking via formation of a water bridge between imidazole nitrogen and pyridyl nitrogen. This contention has helped in understanding some of our previous results as well. The fluorescence spectrum of 2PBI in native nafen exhibits a single band at 450 nm, as the only emitting species is the tautomer form. However, in native membranes the dicationic form exists in the ground state, which is accounted for by the high acidity of nafen membrane. The fluorescence decays recorded across the range of the fluorescence spectrum are not significantly different. The temporal parameters obtained showed the presence of a 2.5 ns and a 5 ns component with almost equal contribution throughout the spectral window. The decays do not exhibit a rise time. Nor are they associated with any component with life times close to 1 ns or 60 ps, which correspond to the lifetimes of  $\text{C}^*$  and  $\text{N}^*$  state, hence the primary pathway of formation of  $\text{T}^*$  must be via deprotonation of dication.<sup>15,16</sup> The ESPT in 2PBI has been studied in restricted media like micelle,<sup>17</sup> reverse micelle,<sup>18</sup> and cyclodextrins.<sup>19</sup> ESPT is hindered in hydrophobic environments of cyclodextrins and in SDS micelles an enhanced ESPT followed by slow solvation of the  $\text{T}^*$  is observed. Similar enhancement of ESPT was slow dynamics of  $\text{T}^*$  in aerosol OT reverse micelle was encountered. With this background, the spectral and temporal features of 2PBI have been explored in dried nafen membrane. This has been manifested in understanding the

microenvironment and dynamics of proton transfer in these membranes.

## ■ EXPERIMENTAL SECTION

Nafion 117 membranes and 2,2'-(pyridyl)-benzimidazole were purchased from sigma Aldrich. The dye is recrystallized from hexane prior to use. The membranes are cleaned by heating with 5%  $\text{H}_2\text{O}_2$  solution for 3 h, followed by rinsing in double distilled water and then heating in 1 M  $\text{HNO}_3$  solution for three hours. This procedure is repeated until transparent membranes are obtained. The acid-treated membranes are suspended in 1 M NaOH solution for 24 h for obtaining cation-exchanged membranes. The excess of salt on the surface is removed by rinsing the membrane with water. The dye is loaded in from an aqueous solution 2PBI (of absorbance  $\sim 1$ ) until the absorbance of membrane was about 0.5. The excess of dye on the surface is removed by rinsing with water. The membranes of lower water content are obtained by heating the membrane in vacuum at 70 °C until no change in weight of membranes was observed. The dried membranes are kept in a nitrogen environment during the course of the experiment to avoid uptake of water by the membranes from the atmosphere. The hydrated membrane had  $\sim 10\%$  w/w water as this is the weight lost upon drying. This corresponds to a  $\lambda = 6$  in hydrated membranes and  $\lambda = 1$  in less hydrated membranes.<sup>20</sup> It may be noted that complete removal of water from nafen membranes is never possible.

The steady state absorption spectrum is measured in JASCO V530 absorption spectrophotometer and fluorescence spectrum is recorded in Varian Cary Eclipse spectrofluorimeter. The time-resolved experiments are performed in IBH Horiba-JY fluorocube. The decays are recorded at magic angle. The sample is excited by Nanoled emitting at 295 nm (fwhm = 700 ps). The membrane is kept at 45° to the excitation source such that the excitation light is directed opposite to the detector, and fluorescence is collected from the back surface of the membrane. The data obtained is fitted to multiexponential models by DAS 6.2 data analysis software using an iterative reconvolution technique. To construct the time-resolved emission spectra (TRES), the decays have been recorded at suitable intervals throughout the range of the fluorescence spectrum. The fitted fluorescence decay has been scaled with steady state spectrum following usual procedure.<sup>21</sup> The spectra thus generated are normalized to unit area to generate time-resolved area normalized emission spectra (TRANES).<sup>22,23</sup> The existence of two state equilibrium in the excited state is followed using TRANES analysis. The TRANES curves are constructed by generating intensity at various times. For the same, the fluorescence decays are recorded at suitable intervals of emission spectra, the temporal parameters obtained by reconvolution are incorporated in the following relationship, and the time-resolved emission spectra is obtained.

$$I_{(t,\lambda)} = I_{(ss,\lambda)} \frac{\sum_i e^{-t/\tau_i^{(\lambda)}}}{\sum_i a_i^{(\lambda)} \tau_i^{(\lambda)}}$$

Where  $I_{(t,\lambda)}$  is the calculated intensity at time  $t$  after excitation.  $\tau_i$  represents the fluorescence lifetime of  $i$ th component and  $a_i$  denotes the contribution of that component at the wavelength at which decays are recorded. A negative value of  $a_i$  indicates a growth in fluorescence intensity with time  $I_{(ss,\lambda)}$  is the time integrated intensity at that wavelength. The traces so obtained are area normalized to obtain TRANES.

The ground state geometries of dication and tautomer are optimized using B3LYP/6-311+G\*\* basis set. The rotational barrier for the rings was devised by optimizing the geometry of the molecule at different angles by rotation of the imidazole group with respect to the pyridyl group using the same basis set at the same level of theory. The first excited states are optimized using time-dependent density functional theory calculations. All of the calculations were performed using the *Gaussian09* package.<sup>24</sup>

## RESULTS AND DISCUSSION

As has been discussed already, the absorption spectrum of 2PBI in native nafen membrane is that of the dication (D) and the fluorescence spectrum is that of the tautomer (T\*), formed by the loss of one of the benzimidazolium protons in the excited state D\*. Upon drying, the absorption spectrum gets red-shifted by 10 nm (Figure 1) indicating that the fluorescent

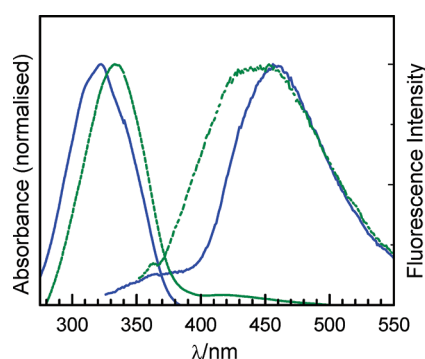


**Figure 1.** Steady state spectra of 2PBI in nafen membranes at two different levels of hydration ( $\lambda = 1$ , green dashed line and  $\lambda = 6$ , solid blue line).

probe molecule experiences a more acidic environment upon drying.<sup>14</sup> A concomitant blue shift in the fluorescence spectrum is observed. This is explained later in the light of time-resolved studies. Thus, the steady state spectra exhibit small but perceptible changes, indicating that the photophysics of 2PBI is affected upon drying the membrane, albeit to a lesser extent than coumarin 102.<sup>11</sup> Time-resolved fluorescence experiments have been performed to examine this effect more closely. The experiments performed in ref 15 have been repeated back to back with the present experiments performed on dried nafen membranes for the sake of comparison (Figures 2 and 3, Table 1). For the membranes with  $\lambda = 6$ , there is hardly any dependence of the dynamics on the wavelength of emission, which is in agreement with the earlier report.<sup>15</sup> Upon drying the membrane to  $\lambda = 1$ , the decays become slower and a strong wavelength dependence sets in. The decays at longer wavelengths are distinctly slower than those at shorter wavelengths (Figure 2). Upon fitting the decays to a biexponential function, a long component is observed at all wavelengths of emission, with its magnitude and contribution increasing with increase in the emission wavelength. A short component, similar to one of the components observed in the hydrated membrane, is present but contributes to a lesser extent. (Figure 2, Table 1). This observation might be explained in two different ways. First, the wavelength dependence of the fluorescence decays could be a result of slow solvation that is typical of microheterogeneous media.<sup>25</sup> It may be argued that the fraction of bound water increases upon drying and this is what brings about the slow solvation dynamics.<sup>26</sup> The other possibility

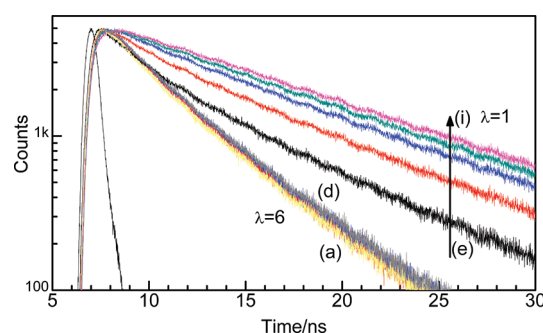


**Figure 2.** Fluorescence decays of 2PBI in nafen membranes at different hydration levels and different emission wavelengths.  $\lambda_{em} =$  (a) 400 (b), (c) and (d) 570 nm,  $\lambda = 6$ .  $\lambda_{em} =$  (e) 380 nm, (f) 420 nm, (g) 460, (h) 490, and (i) 530 nm,  $\lambda = 1$ . The data presented in (a)–(d) are in agreement with that reported earlier (ref 15) and is presented here for the sake of comparison.

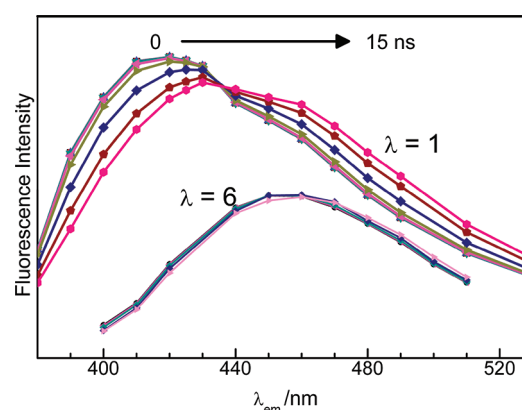


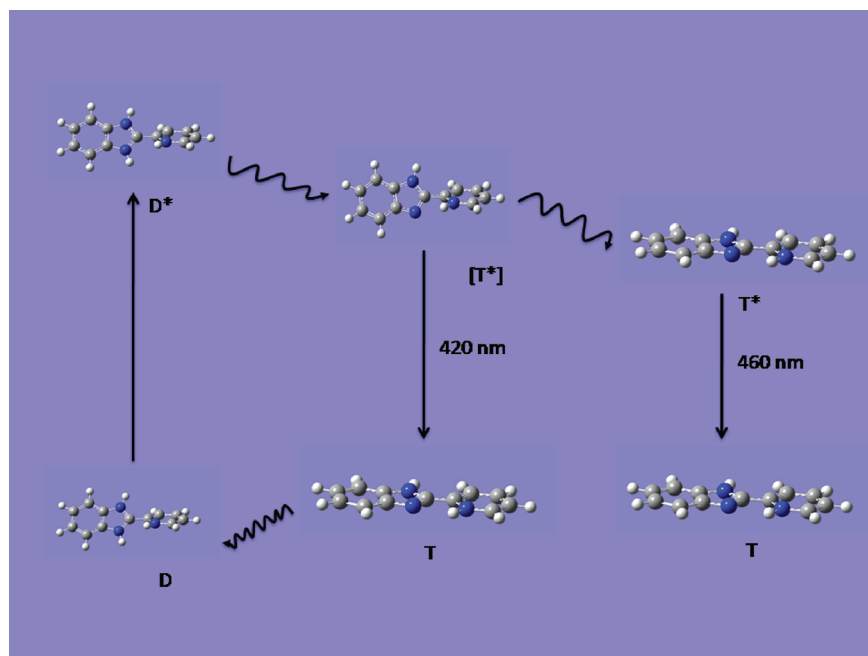
**Figure 3.** TRANES of 2PBI in native nafen membrane at different hydration levels over 15 ns. Upper panel: the green curve is the calculated spectrum at time zero. The red-shifted magenta curves connected by hexagons represent the time evolved spectra after 15 ns. Lower panel: The TRANES spectra of 2PBI over 15 ns in hydrated membrane ( $\lambda = 6$ ). There are no time evolutions, hence all spectra are bunched.

**Table 1.** Temporal Parameters of 2PBI in Native Nafen

$\lambda_{em} / \text{nm}$	$\lambda = 6$				$\lambda = 1$			
	$\tau_1 / \text{ns}$	$\tau_2 / \text{ns}$	$a_1$	$a_2$	$\tau_1 / \text{ns}$	$\tau_2 / \text{ns}$	$a_1$	$a_2$
380					2.06	7.15	0.44	0.55
420	1.78	4.44	0.42	0.58	2.71	8.91	0.31	0.68
460	2.01	4.57	0.42	0.58	3.74	10.0	0.19	0.80
490	2.17	4.70	0.44	0.56	0	9.95	0	1
570	1.95	4.56	0.37	0.62				

is that of an excited state process involving two discrete states. The method of time-resolved area normalized emission spectroscopy (TRANES) is found to be useful to resolve a situation like this, as an isoemissive point in the TRANES arises when there is an involvement of two discrete states. Such an isoemissive point is not observed in case of dynamic solvation.<sup>22,23</sup> The time-resolved emission spectra of 2PBI in the hydrated membrane exhibit a maximum at 460 nm at all times (Figure 3). However, the spectra in the less hydrated membrane exhibit marked time dependence. The maximum at zero time is at 420 nm. It might be worth mentioning here that the zero time spectrum represents the spectrum of sample just after the

Scheme 2. Conformational Relaxation in 2PBI during Deprotonation of the D\* to Give T\*



excitation, before any relaxation process has occurred, which may lead to a time-dependent Stokes shift. With progression in time, the spectra exhibit a dynamic red shift and a prominent shoulder develops at 460 nm, which is same as the position of the maxima in the hydrated membrane. A distinct isoemissive point is observed at 438 nm (Figure 3). Thus, the TRANES indicate the involvement of two emissive states at lower levels of hydration of nafion. It should be noted here that there is no signature of the C\* or N\* states, in the steady state spectra, values of the lifetimes, or in TRANES. So, the two emissive species should be assigned to T\* states, in two different kinds of environments. In fact, the long component observed previously in the hydrated membrane has been assigned to T\* in less polar microenvironment.<sup>15</sup> The contribution and lifetime of this component is found to increase significantly upon drying, indicating a greater partitioning of 2PBI in less polar environments. Such an assignment is in line with the observation of a greater microheterogeneity experienced by coumarin 102 in dried nafion membranes.<sup>11</sup> However, a less polar environment is not the only change that is manifested in the TRANES. The position of the emission spectrum at time zero is worth careful attention as well. It occurs at 420 nm, which corresponds to too high an energy for the T\* emission and too low an energy for the C\* or N\* emission. Contribution from C\* or N\* can be ruled out, as has been discussed already. This blue-shifted emission cannot be assigned to T\* molecules in a less polar environment either, as the long lifetime, characteristic of such species, predominates the red and not the blue edge of the fluorescence spectrum. So, the only option is to assign the initial, blue-shifted emission to T\*, produced in a state of higher energy than usual. One way of this to be achieved is as follows: It is possible that the ground state of the dication, D, exists as a distribution of conformers. If this is the case, then the locally excited D\* would also be produced in a similar distribution of conformations, as has been proposed earlier, for C and C\*.<sup>27</sup> Now, as the T\* state is formed by deprotonation of D\*, it is produced as a distribution of conformations as well. Because the nonplanar conformations of T\* are likely to be

more energetic than the planar structure, they are expected to emit in higher energy than the conformationally relaxed T\* states. Thus, the slight broadening of the steady state fluorescence spectrum and the markedly blue-shifted emission spectrum at initial times, in partially dried nafion, can be rationalized in the light of the early events in the photophysics of the T\* form of 2PBI produced in these membranes (Scheme 2). It may be argued that the changes in the fluorescence behavior might come out due to aggregation of dyes because of electrostatic interactions, as suggested in some earlier reports.<sup>28</sup> There are four reasons why we think that aggregation does not take place. First, the concentration of dye is kept is very small (absorbance = 0.2). No aggregation is reported in homogeneous solutions, even at higher absorbances than this. Second, H or J aggregates have distinct absorption features, which do not show up in the present experiment. If the aggregates are random in nature, then one expects to see a broadening of the absorption spectrum. In our study, the only change in the absorption spectrum that is observed is a red shift of 10 nm. There is no significant change in spectral shape. Finally, dye aggregates are generally less fluorescent than monomers,<sup>29</sup> with some notable exceptions where aggregation-induced enhancement of fluorescence<sup>30</sup> is observed in the solid state due to suppression of molecular motions that contribute to nonradiative processes. In the present case, a slight increase in fluorescence is observed. There is no quenching that is usually observed upon aggregation.

Quantum chemical calculations have been performed to test the hypothesis proposed in the previous paragraph. The optimized geometry of D form has the pyridyl and imidazole rings to be in different planes, and the dihedral angle between the two rings is about 41°. It would be expected that the rings would be perpendicular to each other, a condition where the steric interactions are minimum. However, this condition would lead to complete breakdown of conjugation in the system. The optimum dihedral angle of 41° appears to be a trade-off value where the two factors compensate for each other (Figure 4). Because the two rings are at 41° to each other in the lowest



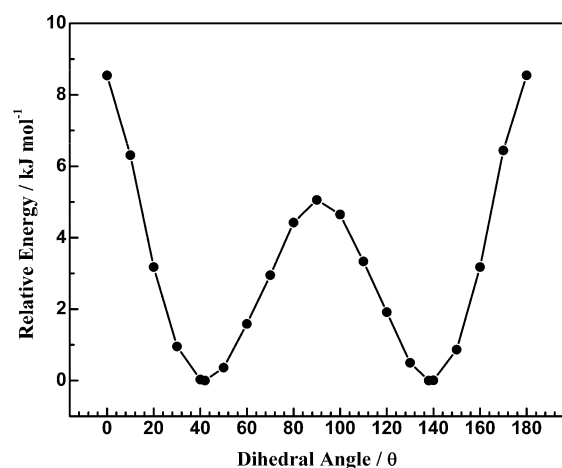


**Figure 4.** Potential energy of 2PBI as a function of the dihedral angle between the planes of imidazole and pyridyl rings.

ground conformation, the Franck–Condon state formed by vertical excitation would also have the two rings oriented at the same angle. This is supported by the TD-DFT calculations as well where the locally excited  $S_1$  state is associated with a dihedral angle of  $41^\circ$  for the dication. Consequently, the  $T^*$  formed by loss of proton is initially in a higher energy, conformationally strained state and would tend to undergo rotation about the bond connecting the imidazole and pyridyl rings during its lifetime. We conclude that at high water content this rotation is ultrafast and the emission is entirely from conformationally relaxed  $T^*$ . However, at lower water contents, the rotation is hindered and it is possible that emission occurs before complete rotational relaxation is achieved. This is manifested in the fluorescence spectrum as a blue shift. As seen from TRANES, the 420 nm band can be assigned to the rotationally strained  $T^*$  form.

Similar experiments have been performed on nafion membranes in which the  $H_3O^+$  ions have been replaced by  $Na^+$  ions and  $(CH_3)_4N^+$  ions. Nafion is an efficient ion-exchange resin and, in the process of ion exchange, a significant amount of water is displaced from the membrane.<sup>6</sup> This is attributed to the size of the cations, which are much larger than the size of water molecules.<sup>15</sup> Our earlier reports have shown that the fluorescent probes 2PBI and coumarin 102 experience a lesser acidity in cation-exchanged nafion membrane, as compared to that in native membranes.<sup>11,15,16</sup> Consequently, in  $Na^+$ -exchanged membranes, 2PBI molecules occur not in the dicationic D form but in the monocationic C and neutral N forms. This is manifested in a blue shift of the absorption maximum to 308 nm. Moreover, the  $C^*/N^*$  emission band at 360 nm, which is absent in the native membrane, is regenerated, giving rise to a dual emission (Figure 5). The characteristic lifetimes of the  $C^*$  as well as  $N^*$  are observed in the blue edge of the emission spectrum while the red edge has contributions from  $T^*$  in regions of different polarities along with a rise time that corresponds to the process of ESPT.<sup>15</sup> The dual emission gives way to a single  $C^*/N^*$  emission at 360 nm upon drying the membrane to  $\lambda = 1$  (Figure 5). However, a very small red shift, possibly marking the loss of water, is the only change that is observed in the absorption spectrum. The near invariance of the absorption spectrum indicates the ground state is the same C/N and not the dicationic D form. So, the effective quenching of the  $T^*$  emission, upon drying, is a result of hindrance of ESPT of 2PBI. Similar observations are made in  $(CH_3)_4N^+$ -

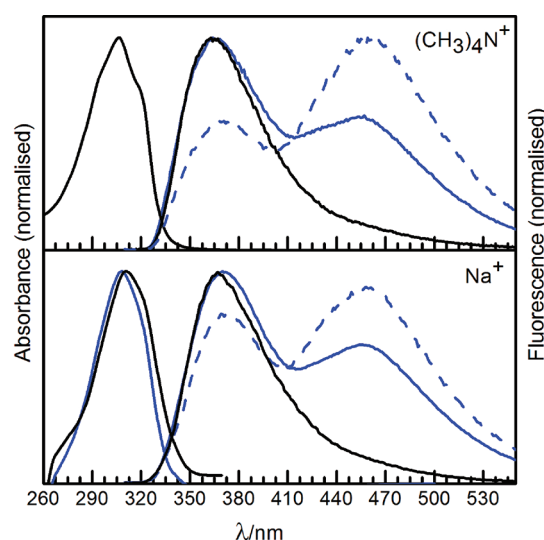


**Figure 5.** Absorption and fluorescence spectrum of 2PBI cation-exchanged nafion membranes at hydration levels of  $\lambda = 6$  (solid blue lines)  $\lambda = 1$  (solid black lines) and fluorescence spectrum of 2PBI in rehydrated membrane (dash blue lines).

exchanged membranes as well (Figure 5). The decays recorded in the blue and red ends of fluorescence in  $(CH_3)_3N^+$ -exchanged membrane at higher water contents overlap with the corresponding decays recorded in  $Na^+$ -exchanged membranes (Figure 6).

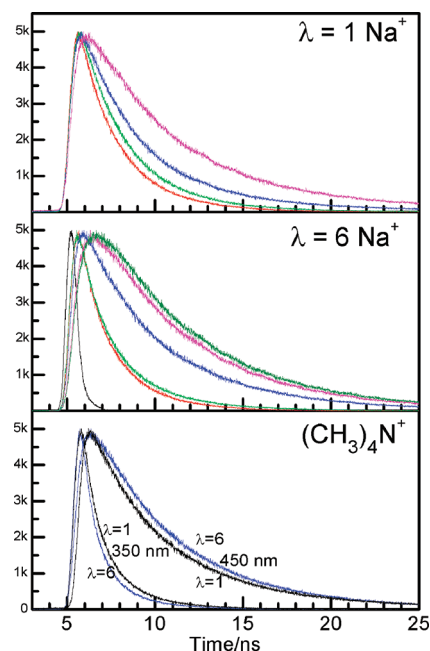


**Figure 6.** Fluorescence decays of 2PBI in cation-exchanged membranes at different hydration levels.  $Na^+$ -exchanged membranes: Top:  $\lambda_{em} = 350, 400, 430$ , and  $470$  nm; middle:  $\lambda_{em} = 350, 400, 430, 470$ , and  $530$  nm,  $(CH_3)_4N^+$ -exchanged membranes; bottom:  $\lambda_{em} = 350$  and  $450$  nm, blue = hydrated, black = dried.

This indicates that the environment experienced by the probe is comparable in both the cases. The steady state fluorescence spectrum shows that the extent of ESPT is less in case of  $(CH_3)_4N^+$ -exchanged membranes. This indicates that the species being probed is the same in both membranes. This is reminiscent of our earlier observation with coumarin 102 in

native nafion membranes.<sup>11</sup> Interestingly, the effect of drying of cation-exchanged membranes is not reflected in the extent of proton transfer of coumarin 102, as it exists in the neutral zwitterionic form in these membranes and does not undergo excited state proton transfer.<sup>11</sup> 2PBI exists predominantly in the cationic (C) form in the sodium-exchanged membrane and can undergo proton transfer in these membranes as well. Thus, this fluorescent probe allows us to extend our study of proton mobility in nafion to cation-exchanged membranes.

The time-resolved experiments support the contention that very small amplitude of 0.22 is observed for T\* at lower hydration levels in Na<sup>+</sup>-exchanged nafion membranes (Figure 6, Table 2). However, in the hydrated membranes, the amplitude

**Table 2. Temporal Features of 2PBI in Dried Na<sup>+</sup>-Exchanged Nafion Membranes**

$\lambda_{\text{em}}/\text{nm}$	$\tau_1/\text{ns}$	$\tau_2/\text{ns}$	$\tau_3/\text{ns}$	$a_1$	$a_2$	$a_3$
350	0.47	2.33		0.43	0.57	
400	0.30	2.21	4.09	−0.49	1.13	0.36
430	0.32	2.62	5.57	−0.80	1.23	0.57
470	0.48	4.73	11.35	−0.94	1.73	0.22

of T\* is as high as 1.80.<sup>15</sup> The blue edge has contributions from a 0.47 ns component and a 2.33 ns component. These may be assigned to the C\* and T\* species, respectively. The reason for the assignment of the shorter component to C\* is that the red edges of the fluorescence spectra exhibit risetimes of the same magnitude, indicating that the species emitting in the red evolves in time from the species emitting in the blue and the T\* state is known to evolve from the C\* state. The third component that shows up in the red edge of the spectrum is a long one, of 4–10 ns. This component is assigned to T\* in the less polar regions of nafion, as discussed earlier.<sup>15</sup> Thus, the time-resolved fluorescence study reveals the occurrence of ESPT in the Na<sup>+</sup>-exchanged membrane even at  $\lambda = 1$ , albeit to a much lesser extent than at  $\lambda = 6$ .

The hindrance to ESPT in the cation-exchanged membrane is reminiscent of the similar observation in native membranes using coumarin 102 in native membranes.<sup>11</sup> In that case, the hindrance to ESPT has been rationalized in the light of a greater restriction to the mobility of the protons, due to enhanced electrostatic interaction with the sulfonate groups, at lower water content. In the case of 2PBI, however, the proton transfer involves one water molecule, at most.<sup>12</sup> It is surprising that the mobility of the cation is restricted even over such miniscule lengths. The observation may be rationalized, in a way similar to that used in ref 11. The cation, C, is expected to be drawn close to the negatively charged sulfonate groups of nafion. This region contains a high fraction of so-called bound water molecules that are strongly hydrogen bonded to the sulfonate groups and hence are immobilized to a large extent. These water molecules are not able to promote the ESPT from C\* to T\* form. This is why the process is hindered at lower levels of hydration. The steady state and time-resolved spectrum of the dried (CH<sub>3</sub>)<sub>4</sub>N<sup>+</sup>-exchanged membranes show interesting feature. The steady state spectrum shows that the ESPT is hindered as no fluorescence peak is seen for the T\* form upon drying the membrane. The fluorescence decays of 2PBI in hydrated and the dried (CH<sub>3</sub>)<sub>4</sub>N<sup>+</sup> membrane overlap with each other. The decays have been recorded across the fluorescence spectrum. This is contrary to what has been observed in Na<sup>+</sup>-exchanged membranes where we observe that the decays are

slower in dried membranes (Figure 6). This is explained as follows. The Na<sup>+</sup> ions are distributed throughout the water pools and hence the C form can interact with the sulfonate groups, thus the electrostatic interactions stabilize the C\* form and the decays are slowed down. However, in the case of (CH<sub>3</sub>)<sub>4</sub>N<sup>+</sup> the increased hydrophobic interaction between the nonpolar methyl group and Teflon backbone leads to a formation of bilayer of nafion and (CH<sub>3</sub>)<sub>4</sub>N<sup>+</sup> ions. As a result, the probe is not able to interact with sulfonate groups and experiences only the bulk water like environment in the water pool. When water content goes down, the probe still observes similar environments as the in case of hydrated membranes and enhanced stabilization that can be provided by the electrostatic interaction between the sulfonate groups and 2PBI is absent. This model is in line with the model proposed by our group in the past.<sup>16</sup> The ESPT is anyway hindered as we move from native membranes to cation-exchanged membranes and it is hindered even more upon drying. At this stage, it should be brought back to attention to the fact stated earlier that proton transfer is hindered even under the circumstances where at most one water molecule is involved.

The dried membranes have been rehydrated by dipping the dried membranes in distilled water. There was no change in absorption spectrum, as may be expected. However, the fluorescence spectrum of 2PBI was different from that of the hydrated membrane, which we had started with (Figure 5). Upon rehydration, the relative amounts of T\* form are higher than that which was there in the membrane prior to drying (Figure 4); or in other words the ESPT from C\* to T\* is enhanced. This observation can be seen as a manifestation of the structural changes that might be taking place because of a hydration-drying-hydration cycle. The drying seems to affect the channels. Subsequently, when the membrane reabsorbs water, the dye molecules get redistributed in such a way that they experience a more waterlike environment and C\*–T\* fluorescence is enhanced. This observation is made in both Na<sup>+</sup> and (CH<sub>3</sub>)<sub>4</sub>N<sup>+</sup>-exchanged membranes and thus does not depend on the nature of cation. Thus, 2PBI not only marks availability of water in cation-exchanged membranes but also indicates the structural changes taking place in the membranes. However, the nature of structural changes cannot be conclusively determined by this experiment.

## CONCLUSIONS

The dye 2,2'-(pyridyl)benzimidazole marks the availability of water and protons in cation-exchanged membranes as well, which our earlier probe Coumarin 102 had failed to do. This is because the dye exists in its cationic form and undergoes ESPT in cation-exchanged membranes, whereas the dye C102 existed as a neutral molecule, incapable of undergoing ESPT. The results are in line with our earlier observations and are indicating that breaking up of water channels may not be the primary governing factor of decrease in proton conductivity with decrease in water content in the nafion membranes. The fluorescent properties behavior of the dye marks the structural changes in the membrane as well.

## AUTHOR INFORMATION

### Corresponding Author

\*E-mail: anindya@chem.iitb.ac.in, Tel: +91-22-2576-7149, Fax: +91-22-2576-3480.

## ■ ACKNOWLEDGMENTS

The authors thank Naval Research Board, India, for a generous research grant to A.D. Senior Research Fellowships from CSIR to E.S.S. and A. Dey are acknowledged gratefully. D.S. thanks DST for an KVPY fellowship. A.K. thanks IIT Bombay for research fellowship. Computational facilities from Computer Centre, IIT Bombay are acknowledged gratefully. A.D. thanks Dr. Pushpito Ghosh for a very useful suggestion.

## ■ REFERENCES

- (1) Bagotsky, V. S. *Fuel Cells*; Wiley, USA, 2008.
- (2) Diat, O.; Gabel, G. *Nat. Mater.* **2008**, *7*, 13–14.
- (3) Mauritz, K. A.; Moore, R. B. *Chem. Rev.* **2004**, *104*, 4535–4585.
- (4) Choi, P.; Jalani, N. H.; Datta, R. *J. Electrochem. Soc.* **2005**, *152*, E84–E89.
- (5) Anantaraman, A. V.; Gardner, C. L. *J. Electroanal. Chem.* **1996**, *414*, 115–122.
- (6) Kreuer, K.-D.; Paddison, S. J.; Spohr, E.; Schuster, M. *Chem. Rev.* **2004**, *104*, 4367–4416.
- (7) Schmidt-Rohr, K.; Chen, Q. *Nat. Mater.* **2008**, *7*, 75–83.
- (8) Gebel, G. *Polymer* **2000**, *41*, 5829–5838.
- (9) Gierke, T. D.; Munn, G. E.; Wilson, F. C. *J. Polymer Sci. Polymer Physics Edition* **1981**, *19*, 1687–1704.
- (10) Lu, Z.; Polizos, G.; Macdonald, D. D.; Manias, E. *J. Electrochem. Soc.* **2008**, *155*, B163–B171.
- (11) Iyer, E. S. S.; Datta, A. *J. Phys. Chem. B* **2011**, *115*, 8707–8712.
- (12) Kondo, M. *Bull. Chem. Soc. Jpn.* **1978**, *51*, 3027–3029.
- (13) Guin, M.; Maity, S.; Patwari, G. N. *J. Phys. Chem. A* **2010**, *114*, 8323–8330.
- (14) Rodriguez-Prieto, F.; Mosquera, M.; Novo, M. *J. Phys. Chem.* **1990**, *94*, 8536–8542.
- (15) Mukherjee, T. K.; Datta, A. *J. Phys. Chem. B* **2006**, *110*, 2611–2617.
- (16) Burai, T. N.; Datta, A. *J. Phys. Chem. B* **2009**, *113*, 15901–15906.
- (17) Mukherjee, T. K.; Ahuja, P.; Koner, A. L.; Datta, A. *J. Phys. Chem. B* **2005**, *109*, 12567–12573.
- (18) Mukherjee, T. K.; Panda, D.; Datta, A. *J. Phys. Chem. B* **2005**, *109*, 18895–18901.
- (19) Rath, M. C.; Palit, D. K.; Mukherjee, T. *J. Chem. Soc., Faraday Trans.* **1998**, *94*, 1189–1195.
- (20) Slade, S.; Campbell, S. A.; Ralph, T. R.; Walsch, F. C. *J. Electrochem. Soc. A* **2002**, *49*, 1556–1564.
- (21) Lackowicz, J. R. *Introduction to fluorescence Spectroscopy*, 3rd ed.; Springer: USA, 2006.
- (22) Koti, A. S. R.; Krishna, M. M. G.; Periasamy, N. *J. Phys. Chem. A* **2001**, *105*, 1767–1771.
- (23) Koti, A. S. R.; Periasamy, N. *J. Chem. Phys.* **2001**, *115*, 7094–7099.
- (24) Frisch, M. J.; Trucks, G. W.; Schlegel, H. B.; Scuseria, G. E.; Robb, M. A.; Cheeseman, J. R.; Scalmani, G.; Barone, V.; Mennucci, B.; Petersson, G. A.; Nakatsuji, H.; Caricato, M.; Li, X.; Hratchian, H. P.; Izmaylov, A. F.; Bloino, J.; Zheng, G.; Sonnenberg, J. L.; Hada, M.; Ehara, M.; Toyota, K.; Fukuda, R.; Hasegawa, J.; Ishida, M.; Nakajima, T.; Honda, Y.; Kitao, O.; Nakai, H.; Vreven, T.; Montgomery, Jr. J. A.; Peralta, J. E.; Ogliaro, F.; Bearpark, M.; Heyd, J. J.; Brothers, E.; Kudin, K. N.; Staroverov, V. N.; Kobayashi, R.; Normand, J.; Raghavachari, K.; Rendell, A.; Burant, J. C.; Iyengar, S. S.; Tomasi, J.; Cossi, M.; Rega, N.; Millam, J. M.; Klene, M.; Knox, J. E.; Cross, J. B.; Bakken, V.; Adamo, C.; Jaramillo, J.; Gomperts, R.; Stratmann, R. E.; Yazyev, O.; Austin, A. J.; Cammi, R.; Pomelli, C.; Ochterski, J. W.; Martin, R. L.; Morokuma, K.; Zakrzewski, V. G.; Voth, G. A.; Salvador, P.; Dannenberg, J. J.; Dapprich, S.; Daniels, A. D.; Farkas, O.; Foresman, J. B.; Ortiz, J. V.; Cioslowski, J.; Fox, D. J. *Gaussian 09*, Revision A. 02; Gaussian, Inc.: Wallingford, CT, 2009.
- (25) Sen Majumdar, S.; Mondal, T.; Das, A. K.; Dey, S.; Bhattacharyya, K. *J. Chem. Phys.* **2010**, *132*, 194505–194513.
- (26) Nandi, N.; Bhattacharyya, K.; Bagchi, B. *Chem. Rev.* **2000**, *105*, 2013–2045.
- (27) Burai, T. N.; Mukherjee, T. K.; Lahiri, P.; Padnda, D.; Datta, A. *J. Chem. Phys.* **2009**, *131*, 34504–34512.
- (28) Moreno-Villoslada, I.; Torres, C.; González, F.; Shibue, T.; Nishide, H. *Macromol. Chem. Phys.* **2009**, *210*, 1167–1175.
- (29) Misra, P. P.; Bhatnagar, J.; Datta, A. *J. Phys. Chem. B* **2005**, *109*, 24225–24230.
- (30) Qian, Y.; Li, S.; Zhang, G.; Wang, Q.; Wang, S.; Xu, H. *J. Phys. Chem. B* **2007**, *111*, 5861–5868.